Contrib Mineral Petrol (1996) 125: 237–250

Y.J. Bhaskar Rao · T.R.K. Chetty · A.S. Janardhan
K. Gopalan

Sm-Nd and Rb-Sr ages and P-T history of the Archean Sittampundi and Bhavani layered meta-anorthosite complexes in Cauvery shear zone, South India: evidence for Neoproterozoic reworking of Archean crust

Received: 5 December 1995 / Accepted: 3 May 1996

Abstract Sittampundi and Bhavani Archean layered meta-anorthosite complexes occur as tectonic lenses within the Cauvery shear zone (CSZ), a crustal scale shear dividing the Precambrian granulite crust of south India into late Archean (> 2.5 Ga) and Proterozoic (c. 0.55 Ga) blocks. They and their host supracrustal-gneiss rocks record at least two stages of tectonometamorphic history. The first is seen as regional scale refolded isoclinal folds and granulite metamorphism (D_1-M_1) while the second stage is associated with dominantly E–W dextral transcurrent shearing and metamorphic recrystallisation (D_2-M_{CSZ}). Whole rock Sm-Nd isochrons for several comagmatic rocks of the layered complexes yield concordant ages: Sittampundi – 2935±60 Ma, ε_{Nd} + 1.85±0.16 and Bhavani – 2899±28 Ma, ε_{Nd} + 2.18±0.14 (2σ errors). Our Sm-Nd results suggest that: (1) the magmatic protoliths of the Sittampundi and Bhavani layered complexes were extracted from similar uniform and LREE depleted mantle sources; (2) M_1 metamorphism occurred soon after emplacement at c.3.0 Ga ago. *P-T* estimates on garnet granulites from the Sittampundi complex characterise the M_{CSZ} as a high-*P* event with metamorphic peak conditions of c. 11.8 kbar and 830°C (minimum). The M_{CSZ} is associated with significant isothermal decompression of the order of 4.5–3.5 kbar followed by static high-temperature rehydration and retrogression around 600°C. The timing of M_{CSZ} is inferred to be Neoproterozoic at c. 730 Ma based on a whole rock-garnet-plagioclase-hornblende Sm-Nd isochron age for a garnet granulite from the Sittampundi complex and its agreement with the 800–600 Ma published age data on post-kinematic plutonic rocks within the CSZ. These results demonstrate that the Cauvery shear zone is a zone of Neoproterozoic reworking of Archean crust broadly similar to the interface between the Napier and Rayner complexes of the East Antarctic shield in a model Proterozoic Gondwana supercontinent.[1]

Y.J. Bhaskar Rao (✉) · T.R.K. Chetty · K. Gopalan
National Geophysical Research Institute,
Hyderabad 500 007, India

A.S. Janardhan
Department of Geology, Manasagangothri,
University of Mysore, Mysore 570 006, India

Editorial responsibility: J. Patchett

Introduction

Anorthosite bearing layered complexes are a common feature of many Archean granulite-gneiss terrains (Ashwal 1993). It has been suggested that their emplacement relates to long term cycles of assembly and break-up of Precambrian supercontinents (e.g. Hatton and Von Gruenewaldt 1990). In this context, the emplacement ages of Archean anorthosite complexes are relevant to models of Precambrian crustal evolution. In general, whole rock Sm-Nd isochrons have yielded reliable emplacement ages for many deformed and metamorphosed Archean layered complexes (e.g. DePaolo 1988; Fletcher et al. 1988; Ashwal and Myers 1994), whereas Sm-Nd and Rb-Sr whole rock-garnet isochrons have been related to prograde and retrograde metamorphism (e.g. Cohen et al. 1988; Mezger 1990; Christensen et al. 1994; Hensen and Zhou 1995). We present here whole rock and mineral Sm-Nd isochron ages and metamorphic *P-T* estimates for the Sittampundi and Bhavani layered anorthosite bearing mafic–ultramafic complexes of Salem and Periyar districts, Tamil Nadu, S.India. These two complexes occur as highly deformed, metamorphosed and dismembered bodies within an extensively exposed mid-crustal shear zone, the Cauvery shear zone (CSZ) in the Precambrian granulite-gneiss terrain of South India (Fig. 1).

Previous studies of the Sittampundi complex (Subramanian 1956; Ramadurai et al. 1975; Janardhan and Leake 1975) and the Bhavani complex (Selvan 1981) described the well developed association of stratiform chromitite with calcic meta-anorthosite ($An_{90\pm3}$) simi-

[1] Mineral symbols are as in Kretz 1983

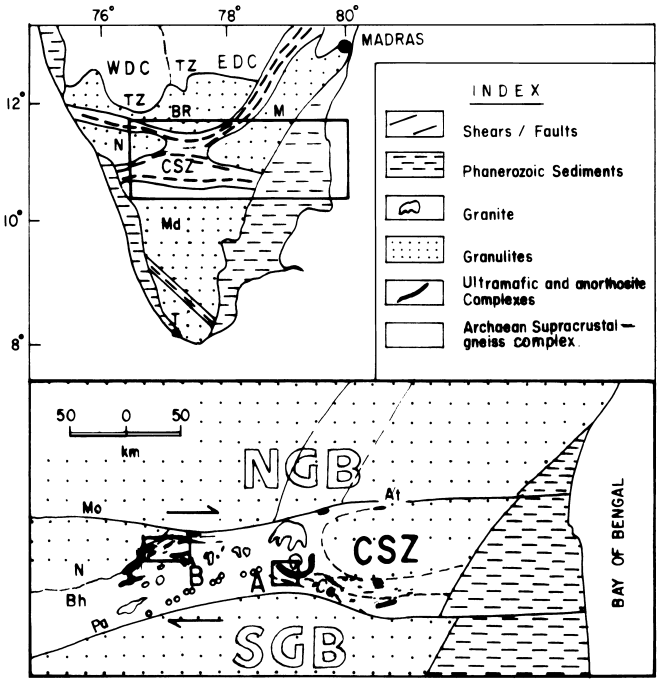

Fig. 1 Geological sketch map showing the Cauvery shear zone (*CSZ*), the Sittampundi complex (*A*) and Bhavani complex (*B*) within the Precambrian granulite terrain of south India. The CSZ is bounded by Moyar (*Mo*), Bhavani (*Bh*), Attur (*At*), Palghat (*Pa*) and Cauvery (*Ca*) shear belts and divides the granulite terrain into northern granulite blocks (*NGB*) including the Nilgiri (*N*), Biligiri Rangan (*BR*) and Madras (*M*) blocks and southern granulite blocks (*SGB*) including the Madurai (*Md*) and Trivandrum (*T*) blocks. *TZ* is a zone of metamorphic transition between the NGB and the western and eastern parts of the Dharwar craton, (*WDC* and *EDC*) respectively

lar to many Archean layered intrusions elsewhere (e.g. the Fiskenaesset complex, W. Greenland; Windley et al. 1973). However, it is now well known (Ashwal 1993) that the Sittampundi and Bhavani complexes present a rather uncommon tectonic setting which is distinctly cratonic akin to some rare occurrences such as the Messina complex, Limpopo mobile belt, S. Africa (Barton et al. 1979). Assuming an Archean age for the Sittampundi and Bhavani complexes, earlier workers proposed a comagmatic evolution of the ultramafic and mafic lithologies in each suite prior to their granulite facies metamorphism at 8–10 kbar, 850°C followed by retrogression related to shearing in the CSZ. However, the chronologies of emplacement, metamorphism and retrogression remain poorly constrained.

Interpretations of the tectonic significance of the CSZ are also ambiguous. The CSZ (referred to by some authors also as the Palghat-Cauvery shear) is a c. 400×80 km, E–W aligned tract of intense ductile shearing, considered by many to form the southern margin of the Dharwar Craton (Ramakrishnan 1993). This zone divides the south Indian granulite terrain into temporally distinct blocks, namely the Archean (≥ 2.5 Ga) northern granulite blocks (NGB) and the southern granulite blocks (SGB) that record a Neoproterozoic (Pan African) granulite imprint at c. 550 Ma (Fig. 1). The CSZ is believed to be a deeply dissected section of an ancient orogenic belt such as the central part of the Limpopo mobile belt, S. Africa (Ramakrishnan 1993). Others have interpreted the CSZ as: (1) a dextral transcurrent shear belt (Drury and Holt 1980); (2) a collapsed marginal basin (Drury et al. 1984); (3) a collision and cryptic suture (Gopalakrishan et al. 1990 ; Ramakrishnan 1993); (4) a prominent terrane boundary linked to the one separating the Archean Napier and Proterozoic Rayner complexes, Enderby Land, E. Antarctica (Harris et al. 1994); (5) a west-directed thrust zone (Chetty and Bhaskar Rao 1996). Much of this ambiguity is due to poorly constrained ages of rocks within the CSZ and their relationship to the adjoining NGB and SGB. The geochronological and geothermobarometric data presented here are expected to not only constrain the time of emplacement and metamorphism(s) of Sittampundi and Bhavani layered complexes, but also contribute to a better understanding of the tectonic evolution of the CSZ.

Regional geology

Granulite terrain of S. India

Recent geological and geochronological data on the granulite-gneiss terrain of S. India have been summarized by Drury et al. (1984), Peucat et al. (1989, 1993), Harris et al (1994), Janardhan et al. (1994) and Jayananda et al. (1995). Granulite blocks north of the CSZ (NGB, Fig. 1) are largely composed of late Archean rock units. Peucat et al. (1989 and 1993) proposed that much of this region is composed of "syn-accretion" charnockite formed by the metamorphism of juvenile calc-alkalic granitoid plutons emplaced at c. 2.5 Ga. Their generation is ascribed to the late Archean subduction related crustal thickening (Drury et al. 1984) or to processes related to mantle plume activity (Peucat et al. 1989). The Sm-Nd evidence for the involvement of older (up to c. 3.4 Ga) protoliths has been obtained for the enderbites and mafic granulites of Biligiri Rangan hills (cf. Janardhan et al. 1994) and also charnockite gneisses along the zone of amphibolite-granulite transition (TZ) (age data summarised by Peucat et al. 1993) at the southern margin of the low to medium grade Dharwar granite-greenstone terrain (WDC and EDC, Fig. 1). The occurrence of older granulites (c. 2.9 Ga) is however, not yet established unequivocally (Mahabaleswar et al. 1995). The Rb-Sr biotite (cooling) ages for granitoid rocks both from the NGB and WDC are c. 2.0 ± 0.1 Ga and plausibly date the stabilization of the Archean crust (Bhaskar Rao et al. 1992; Peucat et al. 1993). There is a record of anorogenic carbonatite-syenite, alkalic ultramafic and alkalic-calc alkalic granite magmatism dated around 800-600 Ma both within CSZ and the NGB (Anil Kumar and Gopalan 1992; Subba Rao et al. 1994; Reddy et al. 1995). In contrast to the NGB, the SGB records an imprint of high grade metamorphism dated at c. 550 Ma, but the ages of the protoliths of these granulites based on Sm-Nd model (T_{DM}) ages are late Archean to Palaeoproterozoic, 2.8–2.1 Ga (Choudhury et al. 1992; Harris et al. 1994; Jayananda et al. 1995).

The Cauvery shear zone

The CSZ shows dominantly ENE–WSW trending axial planar fabrics and easterly plunging sub-horizontal stretching mineral lineations, particularly along a network of shear belts (Chetty and Bhaskar Rao 1996). It exposes an extensive association of high to medium grade supracrustal rocks and Opx-free quartzofeldspathic

gneisses with abundant sheets of granite. The supracrustal formations include largely metasediments (pelites, calc-silicates and marbles, ferruginous quartzite and quartz-rich arenites), which have a distinct platformal character. Metabasic rocks (para- and ortho-amphibolites, mafic granulites) are also abundant. The Sittampundi and Bhavani layered complexes occur as structurally concordant lenses and sheets within the supracrustal-gneiss formations (Fig. 1). This suggests their emplacement into the distinctly cratonic setting quite early in the regional deformation/metamorphic history. The high grade supracrustal-gneiss units and the ultramafic-mafic complexes are interthrust with charnockite-enderbite gneisses.

As summarized by Drury et al. (1984), Gopalakrishnan et al. (1990) and Chetty and Bhaskar Rao (1996), broadly a two stage tectonic development for the CSZ is evident from geological relationships. During the first stage, D_1 (late Archean), large scale fold interference structures developed as the early folds (F_1) were co-axially refolded into tight isoclinal folds (F_2) and upright-open cross folds (F_3). High grade metamorphism (M_1) outlasted F_2. The predominant structural trend of ENE–WSW axial planar mylonitic foliation is due to reworking during the second stage, D_2. This stage is also manifested by the development of a network of shear belts, the loci of retrogression and migmatization. The shear belts (Fig. 1), particularly along the boundaries of CSZ, are associated with significant tectonic transport. For instance, along the Bhavani shear, a dextral displacement of 60–80 km was inferred by Drury and Holt (1980). The *P-T* conditions and timing of a second medium- to high-*P* metamorphism (referred to hereafter as M_{CSZ}) related to $D_2$are less known. A Grt-Cpx-whole rock Sm-Nd isochron age of 2013 ± 16 Ma was reported by Snow and Basu (1986) for a garnet granulite from the Sittampundi complex and interpreted as the time of ecologite facies metamorphism. The Sm-Nd data of four other samples including two anorthosites from the complex (kindly provided by Prof. A.R. Basu) show a large scatter. This large scatter, presumably due to open system behaviour of the very small sample size, precludes any meaningful inference about their time of emplacement.

Sittampundi and Bhavani complexes: previous work

Generalized geology of the two layered complexes is shown in Fig. 2. The Sittampundi complex is composed predominantly of meta-anorthosite gneiss, >90% Pl of $An_{90\pm3}$, and the Bhavani complex of metagabbro and meta-anorthositic gabbros, 60–80% Pl. In general, the rocks show a granoblastic polygonal microtexture. Disequilibrium textures such as symplectitic coronas are common, especially in the metagabbroic rocks containing Grt (Subramanian 1956; Janardhan and Leake 1975; Selvan 1981). Overprinting by retrograde hydrous minerals such as amphibole, clinozoisite and biotite is commonly quite extreme. Relict primary igneous textures and structures such as cumulate and compositional phase layering have been recognized in places, permitting reconstruction of a generalized internal stratigraphy by Ramadurai et al (1975) for the Sittampundi complex and Selvan (1981) for the Bhavani complex. Accordingly, the Sittampundi complex comprises (from bottom upwards) metagabbro-metapyroxenite to Hbl-meta-anorthosite interlayered with chromitite to Czo-meta-anorthosite. This gradation is consistent with major and trace element distributions and variations described by Janardhan and Leake (1975). Rocks described as eclogites by Subramanian (1956) have been redefined as garnet granulites formed at no higher than 10 kbar and 850°C (Janardhan and Leake 1975). Based on field relationships, Selvan (1981) suggested that the Sittampundi and Bhavani suites could be vestiges of a single large intrusive complex. An Archean age for the Sittampundi and Bhavani complexes was assumed in correlations of the host supracrustal-quartzofeldspathic gneiss units with the Archean (≥ 3.0 Ga) Sargur Group and Peninsular gneiss of WDC (Gopalakrishnan et al. 1975 and 1990).

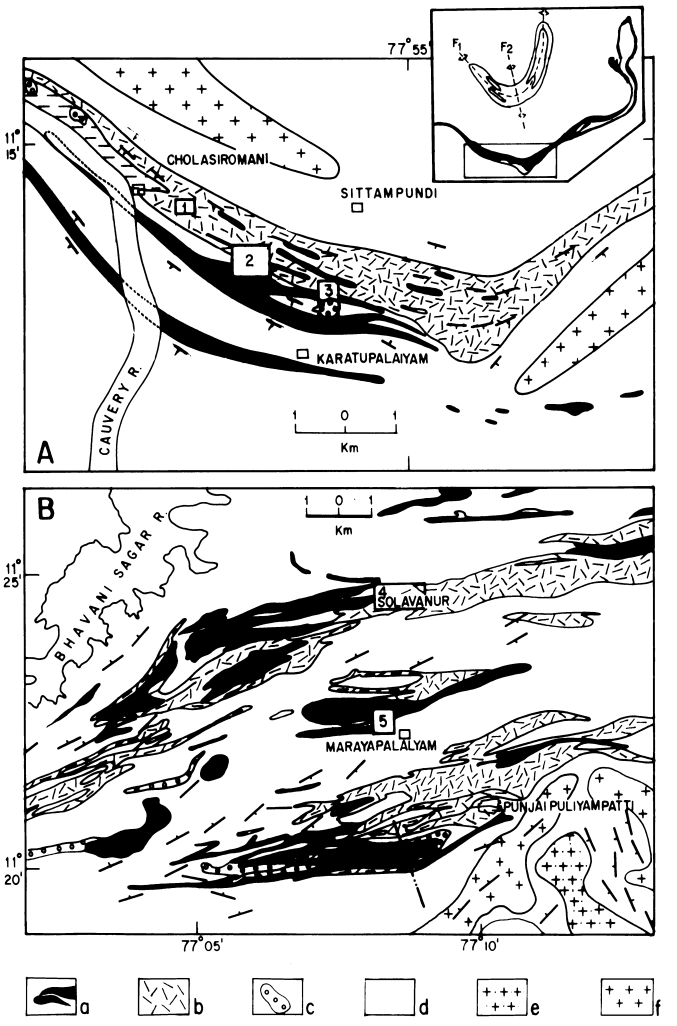

Fig. 2 Generalised geology of parts of the Sittampundi complex (**a**) after Subramanian (1956) and the Bhavani Complex (**b**) after Selvan (1981). *Inset* in **A** shows the general out-crop pattern and structure (after Ramadurai et al. 1975). Major map units are: meta-anorthosite - gabbro (*a*), Grt two pyroxene granulites and ultramafites (*b*) and metapyroxenite (*c*), the high to medium grade supracrustal rocks and migmatitic gneiss complex (*d*) granite gneiss (*e*) and younger granite (*f*)

Sampling and analytical techniques

Fresh samples typically 8–10 kg and a few of ~1 kg were collected mostly from sites of recent excavation (wells, channels or pits). Cluster sampling within a few localities (Fig. 2) ensured representation of small (< 1 m) and large scale (hundreds of metres) compositional variations. The Sittampundi samples were drawn mostly from the limb of a large isoclinal anticline along the southern part of the complex and represent the lower-middle stratigraphic section of Ramadurai et al. (1975). With the exception of 92SLM-87, all samples are from locations 2 and 3, across the strike of compositonal layering in metagabbro and meta-pyroxenite grading to meta-anorthosite through meta-anorthositic gabbro and metagabbroic anorthosite (80-90% Pl). Thus, at location 2, the distance between individual samples varied from < 1 m to ~250 m.

Whole rocks (wr) were powdered in a steel jaw crusher and swing mill. Minerals were hand picked from –60, +80 mesh fractions under a binocular microscope. Major and trace element analyses are by XRF (fused beads) and ICP-MS with an accuracy

of ~3% and 6–7% respectively (Bhaskar Rao et al. 1992). For mineral analysis, a CAMECA (Camebax micro) electron microprobe was used with 15 kV accelerating voltage, 20 nA beam current and a focussed beam of ~1–2 μm diameter. An on-line ZAF correction was used in data processing.

Typically, 100 mg of wr and 50 to 150 mg of minerals (ground to ~200 mesh in an agate mortar) were used for isotopic analysis. Isotopic measurements were on a VG354 thermal ionisation mass spectrometer. The Rb-Sr isotopic measurement procedure has been described by Bhaskar Rao et al. (1992). The Nd and Sm isotopes were analysed as metal ions as described in Anil Kumar et al. (in press). Information on normalization of isotopic ratio data is given in Table 4. Although internal precision on $^{143}Nd/^{144}Nd$ ratios was invariably better, we have quoted an external precision of 2 in the fifth decimal place for the Nd data in Table 4, except as noted. During this study, the mean $^{143}Nd/^{144}Nd$ ratio for La Jolla Nd standard was 0.511861 ± 15 (2σ), $n=11$. The total process blanks for both Nd and Sm are less than 100 pg.

The double error regression method (Williamson 1968) was followed for isochron age calculations using the computer program of Provost (1990), using a blanket error of 0.15% on $^{147}Sm/^{143}Nd$, 1% on $^{87}Rb/^{86}Sr$ and the in-run 1 σ (mean) error for $^{143}Nd/^{144}Nd$ and $^{87}Sr/^{86}Sr$. Decay constants used are 6.54×10^{-12} a^{-1} for ^{147}Sm and 1.42×10^{-11} a^{-1} for ^{87}Rb. Errors in age and initial isotopic compositions reported are 2 σ after multiplication with $\sqrt{}$MSWD mean standard weighted deviates whenever MSWD > 1. The value ε_{Nd} was calculated by the method of Fletcher and Rossman (1982).

Results

Petrography and mineral chemistry

Sample descriptions and locations are given in Table 4 and Fig. 2 and the general scheme of mineral paragenesis in relation to M_{CSZ} is shown in Fig. 3. Meta-anorthosite-gabbroic anorthosites are whitish or pale grey with a distinct gneissic fabric due to flattening of Pl, and in some cases mylonitic due to layer-parallel stretching. Granoblastic polygonal textures with 120° triple junctions between Pl and interstitial Hbl are common, indicating recrystallization under equilibrium conditons. Layer-parallel mylonitization is accompanied by granulation, recrystallization and strain effects on Pl. Besides Hbl, accessory minerals include Czo, Chl, Mag, Ap and Scp. Samples 94SLM-13 and 15 contain Cpx partially replaced by Chl. Sample 92SLM-84 includes up to 4% biotite (by volume) as prismatic and radial plates (0.1–0.5 cm) across foliation. Similar textures for Czo and Chl throughout the Sittampundi and Bhavani suites indicate that retrograde hydration reactions were at static high-*P*-*T* conditions. Some samples contain accessory Grt.

The meta-anorthositic gabbro and metagabbro samples are Hbl-, Pl- and Cpx-bearing. An inequigranular granoblastic habit is distinct in small domains but is largely overprinted by growth of Hbl and Chl. Accessory Mag, Ilm, Rt, Chl, Ap, and sulphides like Py, Po are common. Metagabbros and meta-anorthositic gabbros at locations 2 and 3 contain layers with abundant Grt.

The garnet-granulite samples are variably retrogressed (Figs. 4a,b). Sample 94SLM-50, associated with metapyroxenite-meta-anorthosite at location 3, is among the least retrogressed, preserving relict equigranular granoblastic texture (Fig. 4b), while samples at location 2 (92SLM-77, 83 and 94SLM-58) preserve this texture only in small domains (Fig. 4b). In the latter, large grains of

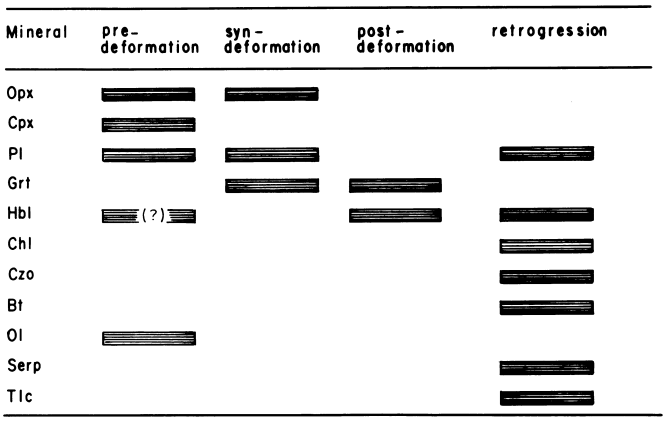

Fig. 3 Summary of mineral paragenesis in relation to D_2-deformation in the Sittampundi and Bhavani layered complexes

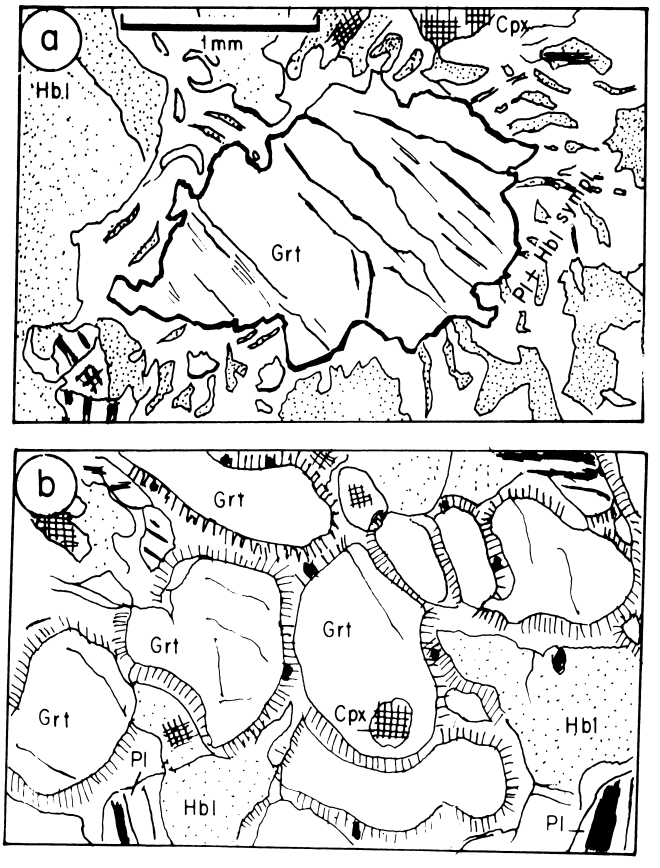

Fig. 4a, b Sketches from photomicrographs of the Sittampundi samples: **a** garnet granulite (metagabbro) 92SLM-83 showing the prominent hornblende-plagioclase symplectite rim around garnet; **b** garnet granulite 94SLM-50 showing better preservation of a granoblastic polygonal habit and thin symplectite rims of Hbl-Pl-Opx-opaques around garnet

Table 1 Representative mineral composition, garnet granulite 94SLM-50 from Sittampundi complex

	Grt		Cpx		Opx		Pl (matrix)		Pl (sym-plectite)	Hbl (matrix)	Hbl (sym-plectite)
	Core	Rim	Core	Rim	Core	Rim	Core	Rim	Core	Core	Rim
SiO_2 (wt%)	39.09	39.46	50.06	50.65	51.87	51.50	55.39	55.65	46.62	44.82	44.00
TiO_2	0.03	0.04	0.18	0.15	0.04	–	0.02	0.06	0.02	0.20	0.25
Al_2O_3	23.37	24.21	6.18	6.59	2.39	2.28	28.70	27.43	33.70	13.90	14.81
FeO	14.87	15.30	5.36	5.44	17.33	17.14	0.01	0.02	0.19	8.54	7.87
MnO	0.37	10.48	0.18	0.10	0.23	0.29	0.03	0.08	–	0.07	0.18
MgO	14.04	13.61	15.56	16.40	28.29	28.30	–	0.03	–	16.97	16.75
CaO	6.70	7.06	20.44	20.22	0.35	0.44	10.07	10.15	16.32	10.77	10.95
Na_2O	0.15	–	0.86	0.97	–	–	6.30	5.75	1.92	2.70	2.95
K_2O	0.05	0.04	0.06	0.05	0.06	0.05	0.07	0.07	0.05	0.08	0.08
Cr_2O_3	0.10	0.07	0.21	0.08	0.04	–	–	–	0.08	0.10	0.10
NiO	0.03	0.01	0.07	0.09	0.01	0.06	–	0.14	–	0.13	–
Cations											
Si	5.838	5.811	1.852	1.841	1.882	1.880				6.383	6.285
Ti	0.003	0.004	0.005	0.004	0.001	–				0.021	0.027
Al^{IV}	4.115	4.204	0.148	0.159	0.102	0.098				2.335	4.494
Al^{VI}			0.121	0.123							
Fe^{2+}	1.857	1.885	0.093	0.071	0.427	0.425				1.017	0.940
Fe^{3+}			0.073	0.094	0.099	0.098					
Mn	0.047	0.060	0.006	0.003	0.007	0.009				0.008	0.022
Mg	3.125	2.987	0.858	0.888	1.530	1.540				2.603	3.566
Ca	1.072	1.114	0.810	0.788	0.014	0.017	0.483	0.492		1.644	1.676
Na	0.638	–	0.062	0.068	–	–	0.547	0.508		0.746	0.817
K	0.010	0.008	0.003	0.002	0.003	0.002	0.004	0.004		0.015	0.015
Cr	0.012	0.008	0.006	0.002	0.001	–				0.011	0.011
Ni	0.004	0.001	0.002	0.003	–	0.002				0.015	–
Number of O	24		6		6		6		8	23	

Table 2 Representative mineral compositions of retrograded garnet granulite 92SLM-83 from the Sittampundi complex

	Grt		Cpx		Pl (matrix)		Pl (symplectite)		Hbl (matrix)	Hbl (sym-plectite)
	Core	Rim	Core	Rim	Core	Rim	Core	Rim	Core	Core
SiO_2 (wt%)	37.08	37.44	51.39	53.00	52.05	55.09	51.34	49.08	44.23	44.81
TiO_2	0.03	0.03	0.11	0.01	–	–	0.02	–	1.43	1.32
Al_2O_3	22.23	22.29	0.75	0.96	29.36	29.98	30.09	32.69	11.17	10.75
FeO	24.85	27.23	10.16	10.46	0.07	0.03	0.01	–	17.85	17.43
MnO	0.88	2.14	0.28	0.30	0.07	–	0.03	–	0.21	0.34
MgO	8.17	4.71	13.41	13.66	0.07	–	–	0.02	10.85	11.18
CaO	6.49	6.73	21.56	21.44	10.82	9.93	12.75	14.32	10.28	10.14
Na_2O	–	–	0.43	0.32	6.41	6.21	4.45	3.35	1.70	1.57
K_2O	0.05	0.03	0.03	0.02	0.06	0.06	0.04	0.04	0.18	0.23
Cr_2O_3	0.62	–	–	0.04	0.02	0.06	0.01	–	0.18	0.08
NiO	–	–	–	0.06	–	–	0.02	–	0.04	0.04
Cations										
Si	5.767	5.866	1.970	1.982					6.584	6.658
Ti	0.011	0.004	0.003						0.16	0.147
Al^{IV}	4.076	4.117	0.030	0.018					1.956	1.883
Al^{VI}			0.004	0.024						
Fe^{2+}	3.232	3.568	0.274	0.312					2.217	2.166
Fe^{3+}			0.052	0.015						
Mn	0.116	0.284	0.009	0.010					0.026	0.043
Mg	1.894	1.100	0.766	0.761					2.402	2.476
Ca	1.051	1.130	0.886	0.859	0.571	0.535	0.628	0.703	1.636	1.614
Na	–	–	0.032	0.023	0.004	0.003	0.397	0.298	0.390	0.452
K	0.010	0.010	0.001	0.001	0.001	0.002	0.002	0.002	0.034	0.044
Cr	0.002	–	–	0.001					0.021	0.009
Ni	–	–	–	0.002					0.005	0.005
Number of O	24		6		8		8		23	

Hbl of two generations overprint a former granoblastic-polygonal texture. The later Hbl replaces Cpx and Grt, and Chl replaces Cpx, early Hbl, Grt and Opx.

Mineral phases of samples 94SLM-50 and 92SLM-83, representing respectively the less and appreciably retrogressed variants, have been analyzed for geothermobarometry. Compositions of some representative mineral phases are summarised in Tables 1 and 2, and described below.

In 92SLM-83, garnet occurs as coarse anhedral and embayed grains, up to 0.5 cm across, in an inequigranular matrix of Hbl+Cpx+Pl and opaques. Garnet is invariably separated from the matrix by a prominent (up to 0.2 mm wide) Pl+Hbl+Mag (± Py) symplectite (Fig. 4a). In places the symplectite has replaced Grt completely leaving moats of Pl+Hbl intergrowth. Garnet is generally free from inclusions except for rare 5–30 μm Ap, Rt and aggregates of rounded embayed Qtz. Garnets in 94SLM-50 are subhedral and near equidimensional. The symplectites in this sample include minor Opx partially replaced by Hbl (Fig. 4b). Garnet is Prp-Alm with a compositonal zoning (particularly prominent in 92SLM-83) marked by Prp depletion, enrichment of mainly Alm and marginally Grs from core to rim. Plagioclase is more calcic in the symplectite than in the matrix. In general, the Cpx (augite), Opx (bronzite) and the amphibole (magnesio hornblende) do not show strong compositional zoning. However, some Cpx and Opx show Al enriched cores relative to rims (Tables 1 and 2). These features are similar to mafic granulites elsewhere that have undergone significant decompression (e.g. Harley 1988; Sandiford et al. 1988; Thost et al. 1991). The symplectite textures are best explained by garnet-breaking reactions during decompression. For instance:

$$\underset{\text{Grt}}{CaMg_2Al_2Si_3O_{12}} + \underset{\text{Qtz}}{SiO_2} = \underset{\text{Pl}}{CaAl_2Si_2O_8} + \underset{\text{Opx}}{Mg_2Si_2O_6}$$

and

$$\underset{\text{Grt}}{MgAl_2Si_3O_{12}} + \underset{\text{Cpx}}{CaMgSi_2O_6} + \underset{\text{Qtz}}{SiO_2} = \underset{\text{Pl}}{CaAl_2Si_2O_8} + 2\underset{\text{Opx}}{Mg_2Si_2O_6}$$

Presence of Qtz inclusions in Grt lends support to the relevance of these SiO_2-consuming reactions. Alternatively, a dehydration reaction such as Grt+Hbl+Cpx =Opx+Pl+ vapour (see Harley 1988) may also be relevant. In either case, the textures and the ubiquitous Hbl in symplectites indicate high-temperature static rehydration possibly during late stage decompression.

Metamorphic conditions

Geothermometry is based on Fe-Mg exchange between coexisting Opx-Cpx, Opx/Cpx-Grt and geobarometry on the Grt-Cpx-Pl-Qtz and Grt-Opx-Pl-Qtz assemblages. In general, these geobarometers use two end member mineral equilibria: (1) Mg end member (P_{Mg}; Pl-Prp-Grs-En-An-Qtz); (2) Fe end member (P_{Fe}; Alm-Grs-Fs-An-Qtz). The assumptions and methods utilized in the derivation of the various geothermobarometric model equilibria involving these assemblages (Table 3) have been summarized recently by Lal (1993), who also proposed new calibrations for the end member equilibria for a simultaneous solution of *P* and *T*. The *P-T* estimates based on calibrations assuming both ideal and non-ideal mixing models are summarized in Table 3. The temperatures are calculated assuming 11 kbar and 7 kbar respectively for 94SLM-50 and 92SLM-83, while all *P* estimates are at $T=750$°C. The Opx-Cpx thermometric calibrations of Lee and Ganguly (1988) and of Raith et al. 1983 (based on Wells 1979) for the granoblastic-textured sample 94SLM-50 give temperatures far in excess of 1000°C while most other calibrations give *T* between 950–750°C on core compositions and 50–100°C lower for rims and symplectite. Based on a preliminary assessment, we believe these anomalously high-*T* estimates may be due to the compositional dependence of the respective equilibrium K_Ds, particularly in terms of the high Ca bulk composition of sample 94SLM-50. For the same sample, Lal's (1993) simultaneous solutions using P_{Fe} and P_{Mg} gives 11.87 kbar and 925°C based on Grt core compositions. This is consistent with estimates from other calibrations. In contrast, sample 92SLM-83 indicates lower equilibration *P* and *T* at < 8.5 kbar and 820–720°C for mineral cores and still lower values (7.5 kbar and $\sim$ 600°C) for rim and symplectite assemblages.

We have also computed *P-T* values by the internally consistent thermobarometric calculations and equilibrium diagrams using Berman's (1991) TWEEQU computer program. We used the updated thermodynamic data set (Berman 1991) and end member solid solution activity models for Grts (Berman 1990; Berman and Koziol 1991), Pl (Fuhrman and Lindsley 1988) and Cpx and Opx (Newton 1983). A *P-T* diagram (Fig. 5) illustrates geothermobarometric equilibria for the granoblastic garnet granulite 94SLM-50 on a volatile-free basis and without hydrous phases, but including equilibria involving Ilm and Rt.

Geothermometry by TWEEQU utilises reactions involving Fe-Mg exchange between Cpx-Grt or both Cpx-Opx and Grt. For instance Alm + 3Di=Prp + 3 Hd and Alm + 6 Di=3Hd + Grs + 3 En. Pressure estimates involve Alb in reactions leading to formation and breakdown of Grt. Some of these reactions are shown in Fig. 5. In essence, two distinct intersections of geothermometers and barometers at variable *P* but broadly similar *T* are obtained (Fig. 5). These intersections constrain *P* and *T* for garnet formation and breakdown quite closely; $A=11.6\pm1.1$ kbar and 654 ± 27°C using 34 out of 107 intersections and $B=7.1\pm0.3$ kbar, 650 ± 23°C from 56 out of 107 intersections. Compared with estimates from other calibrations (Table 3), these intersections indicate lower values for *T*, but more significantly the bimodal nature of *P*. Even assuming the low temperature to be a minimal estimate (reflecting effects of retrogression and development of hydrous phases), the disagreement in the *T* estimates is quite conspicuous. Similar low –*T* estimates elsewhere were explained as either due to the inadequacies in the assumed thermodynamic data and cation

Table 3 Results of geothermobarometric estimates for garnet granulites from the Sittampundi complex

Calibration used	94 SLM-50		92 SLM-83		
	Grt core, matrix Cpx, Opx and Pl	Grt rim, matrix Cpx, Opx and Pl	Grt core, matrix Cpx and Pl	Grt rim, matrix Cpx and Pl	Grt rim, matrix Cpx Sympl. Pl
Geothermometry (°C)	at 11 kbar		at 7 kbar		
Grt-Cpx					
Ellis and Green (1979)	752	664	776	654	665
Ganguly and Saxena (1989)	824	738	853	740	750
Krogh (1988)	690	600	715	590	601
Dahl (1980)			800	638	600
Grt-Opx					
Harley (1984b)	951	906			
Lee and Ganguly (1988)	1111	1065			
Raith et al. (1983)	1239	1142			
Lal (1993)	977	930			
Cpx-Opx					
Powell (1978)	767				
Wells (1977)	1028				
Geobarometry (kbar) at 750° C					
Grt-Cpx-Pl-Qz					
Holland and Powell (1990)	10.29	10.3	6.3	4.74	4.24
Eckert et al. (1991)	12.68	12.79	8.64	7.01	6.49
Holland and Powell (1990) By Eckert et al. (1991)	12.39	12.45	8.42	6.83	6.32
Moecher et al. (1988),					
P_{Mg}	12.16	13.34	8.74	7.76	7.25
P_{Fe}	12.22	14.72	8.58	8.56	8.07
Grt-Opx-Pl-Qz					
Newton and Perkins (1982),					
P_{Mg}	12.09	11.85			
Eckert et al. (1991)	12.16	11.92			
Holland & Powell (1990) By Eckert et al. (1991)	12.1	11.86			
Perkins and Chipera (1985),					
P_{Mg}	10.77	10.56			
P_{Fe}	11.12	11.28			
Moecher et al. (1988)	12.15	12.26			
Bohlen et al. (1983)	11.5	11.47			
Wells (1977) By Raith et al. (1983)	11.86	11.63			
Lal (1993)					
P_{Mg}	11.34	9.02			
P_{Fe}	11.14	9.17			

exchange models for the end member equilibria (e.g. Berman and Aranovich 1993; Kamber et al. 1995) or a 'feed back' of post-peak Fe-Mg equilibration involving Grs or Prp end members in garnet (e.g. Fitzsimons and Harley 1994).

Geochronology

Sm-Nd results on Sittampundi and Bhavani complexes

Isotopic compositions and elemental abundances are given in Table 4 and depicted in a Nd evolution diagram (Fig. 6). The 13 samples analysed show a good spread in $^{147}Sm/^{144}Nd$ from 0.118 to 0.294 and conform closely to a good linear array. If this array is interpreted as an isochron, it corresponds to an age of 2935 ± 60 Ma (MSWD=5.53) and an initial Nd isotopic composition (Nd_i) of 0.50892 ± 0.00007 ($\varepsilon_{Nd} = +1.85 \pm 0.16$). Three samples, 92SLM-77, 81 and 94SLM-50, show a very small deviation from the best fit regression line, which exceeds analytical errors. The reason for this departure is not clear. The agreement between duplicate analyses of these samples suggests the departure may not be due to analytical factors like sample inhomogeneity, incomplete dissolution or Sm/Nd fractionation due to CaF_2-REE complexing (e.g. Korsch and Gulson 1988), but to some unknown geological factor(s). One possibility could be their small size ($\sim$1 kg) relative to the other samples. Exclusion of these samples from the regression

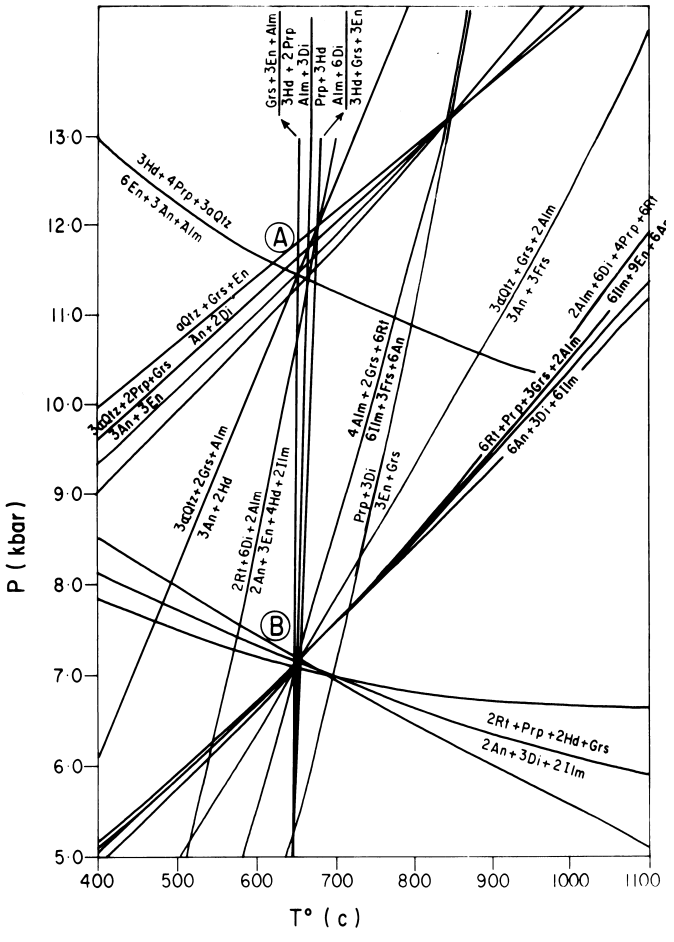

Fig. 5 A simplified *P-T* diagram showing intersections between the geothermometric and geobarometric reaction curves using Berman's (1991), TWEEQU program. Prominent intersections are: $A=11.8\pm1.1$ kbar and $B=7.1\pm0.3$ kbar and ~650°C. Important mineral reactions are labelled

improves the MSWD to 2.07, but the age (2871 ± 46) and Nd_i (0.50898 ± 0.00005) remain the same within error limits. Model T_{DM} ages for most samples with $^{147}Sm/^{144}Nd < 0.18$ range between 2.92–3.07 Ga while the corresponding T_{CHUR} model ages are lower at 2.5–2.7 Ga (Table 4).

Mineral fractions of garnet, hornblende and plagioclase from sample 92SLM-83 (garnet granulite) and hornblende and plagioclase from metagabbro (amphibolite) 92SLM-87 have been analysed (Table 4). In selecting garnets, care was taken to avoid the symplectite shell. Whereas minerals and wr for 92SLM 87 do not define an isochron due to the limited spread in $^{147}Sm/^{144}Nd$, those of 92SLM-83 define a good internal isochron controlled mainly by the garnet (line 2, Fig. 6). This mineral isochron (MSWD=1.63) corresponds to an age of 726 ± 9 Ma and Nd_i of 0.51185 ± 3 [ε_{Nd} (T=725 Ma)$=+2.77\pm0.5$].

Four samples from the Bhavani complex (Table 4) show a good spread in $^{147}Sm/^{144}Nd$ between 0.117–0.198 and yield a well defined isochron age of 2898 ± 52 Ma and Nd_i of 0.50899 ± 6 ($\varepsilon_{Nd}=+2.18\pm0.14$) (Fig. 7).

Rb-Sr results, Sittampundi complex

In general, anorthosites as well as anorthositic gabbros show very little radiogenic Sr enrichment due to their very low Rb (<0.1 ppm) and high Sr (200 to > 1000 ppm). The Rb-Sr data for seven samples are given in Table 4 together with mineral analyses for the two samples described in the previous section. The seven whole rock samples have a very limited spread in $^{87}Rb/^{86}Sr$ between 0.0036–0.115 and plot reasonably well on a straight line corresponding to an age of 2283 ± 308 Ma, and $Sr_i=0.7013\pm2$, (MSWD=19.2). One of the less radiogenic samples, 92 SLM-87, plots off the regression line to the left. Exclusion of this sample from the regression calculation gives essentially the same age and Sr_i of 2119 ± 140 Ma and 0.7015 ± 1 (Fig. 8), but reduces the MSWD significantly to 4.3.

Hornblende and garnet fractions separated from the two whole rock samples 92SLM-87 and 92SLM-83 did not show sufficient difference in their Rb/Sr ratios to define a precise mineral isochron. However, the mineral data of 92SLM-83 fall distinctly away from the whole rock isochron and correspond to an approximate age of 779 ± 360 Ma with a Sr_i of 0.7017 ± 1 (Fig. 8).

Discussion

Time of emplacement and early metamorphism of Sittampundi and Bhavani complexes

An important outcome of this study is that the two layered complexes, spaced about 90 km apart, give concordant Sm-Nd whole rock isochron ages of c. 2.9 Ga; Sittampundi, 2935 ± 60 Ma and Bhavani, 2989 ± 52 Ma. That these linear isotope correlations are *not* mixing lines without any time significance follows from the following considerations.

Chondrite-normalised REE patterns for samples representative of the different lithotypes in the Sittampundi complex are shown in Fig. 9. The REE patterns of all rocks are generally similar, varying only in their total REE. The Sittampundi meta-anorthosites have similar REE abundances and patterns to Archean anorthosites elsewhere, e.g. the Fiskenaesset complex (for comparison, Henderson et al. 1976; Phinney et al. 1988). There is a clear gradation in total REE from metagabbro to meta-anorthosite, with progressively more positive Eu anomalies and similar LREE fractionation. A few gabbros and some garnet granulites show strong LREE depletion and low La_N/Sm_N compared to other comagmatic members of the suite. However, this cannot be ascribed to metamorphism but to primary fractional crystallisation processes as explained by Henderson et al. (1976) for similar trends in the Fiskenaesset gabbros. These observa-

Table 4 Sm-Nd and Rb-Sr isotopic data for Sittampundi and Bhavani samples. Errors on $^{87}Sr/^{86}Sr$ and $^{143}Nd/^{144}Nd$ are 2σ of the mean and correspond to least significant digit. $^{143}Nd/^{144}Nd$ normalized to $^{146}Nd/^{144}Nd=0.7219$. ε_{Nd} (T) at T=2950 Ma. Model ages, T_{CHUR} calculated using $^{143}Nd/^{144}Nd$ CHUR=0.512638, $^{147}Sm/^{144}Nd$ CHUR=0.1967. T_{DM} calculated using the equation of De Paolo (1981)

Sample no.	Loc.[a]	Des.[b]	Rb (ppm)	Sr (ppm)	Sm (ppm)	Nd (ppm)	$^{87}Rb/^{86}Sr$	$^{87}Sr/^{86}Sr$	$^{147}Sm/^{144}Nd$	$^{143}Nd/^{144}Nd$	ε_{Nd} (T)	T_{CHUR} (Ma)	T_{DM} (Ma)
Sittampundi complex													
92SLM-84	(2)	AG	10.4	260.5	3.5	18.1	0.115	0.70496±6	0.1189	0.51206±2			
92SLM-85	(2)	GA	24.7	802.0	4.6	23.5	0.089	0.70423±4	0.1183	0.51122±2	+2.01	2736	2918
94SLM-7	(2)	GA			4.0	20.5			0.1195	0.51127±2	+2.52	2682	2874
94SLM-41	(3)	P			0.1	0.3			0.1394	0.51162±2	+1.92	2675	2923
94SLM-42	(3)	P			1.3	4.9			0.1591	0.51197±2	+1.26	2672	3021
94SLM-26	(3)	Grt. GA			0.2	0.6			0.1685	0.51216±2	+1.38	2550	3017
94SLM-15	(2)	A			0.1	0.4	0.002	0.70165±1	0.1739	0.51227±2	+1.26	2462	3032
92SLM-81	(2)	AG	1.2	136.1	2.7	8.6	0.048	0.70283±8	0.1880	0.51259±2	+2.33		
92SLM-77	(2)	Grt. G	0.4	90.4	2.1	6.4	0.014	0.70182±3	0.2006	0.51284±2	+2.58		
94SLM-13	(2)	AG			0.1	0.3			0.2024	0.51284±2	+1.79		
94SLM-58	(2)	Grt. G			2.5	7.2			0.2051	0.51288±2	+1.53		
94SLM-50	(3)	Grt. AG			0.1	0.3			0.2436	0.51369±2	+2.74		
92SLM-83	(2)	Grt. G	0.4	90.8	2.4	7.5	0.011	0.70175±4	0.2021	0.51281±2	+1.36		
92SLM-83 Grt			0.05	10.2	0.7	0.5	0.013	0.70186±9	0.8508	0.51590±2			
92SLM-83 Hbl			0.3	29.1	3.6	10.6	0.026	0.70201±5	0.2050	0.51270±4			
92SLM-83 Pl			0.1	210.6	0.2	0.9	0.001	0.70172±3	0.1442	0.51239±3			
92SLM-87	(1)	AG	0.3	264.7	0.7	3.5	0.004	0.70170±4	0.1237	0.51133±2	+2.09	2712	2910
92SLM-87 Hbl			1.5	24.3	3.1	12.5	0.178	0.70253±7	0.1480	0.51159±2			
92SLM-87 Pl			0.1	194.3	0.1	0.5	0.001	0.70156±3	0.0648	0.51135±5			
Bhavani complex													
94BH-50	(4)	GA			3.7	29.3			0.1171	0.51123±2	+2.28	2676	2864
94BH-55	(4)	G			3.2	11.6			0.1171	0.51123±2	+2.15	2416	2847
94BH-49	(4)	GA			0.4	1.2			0.1858	0.51254±2	+2.21		
94BH-57	(5)	Grt. G			2.0	6.2			0.1980	0.51278±2	+2.33		

[a] Sample locations (1–5) shown in Fig. 2
[b] Sample description (*A* meta-anorthosite, *Ga* metagabbroic anorthosite, *AG* meta-anorthositic gabbro, *G* metagabbro, *Grt* garnet bearing)

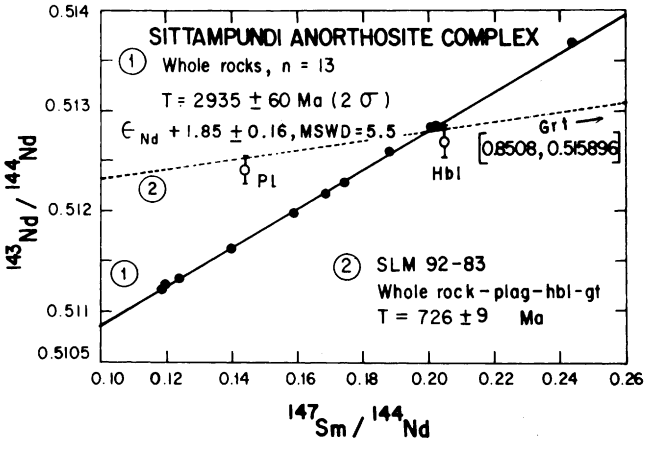

Fig. 6 Nd evolution diagram for the Sittampundi samples. Whole rocks (*1*) and whole rock - minerals (*2*)

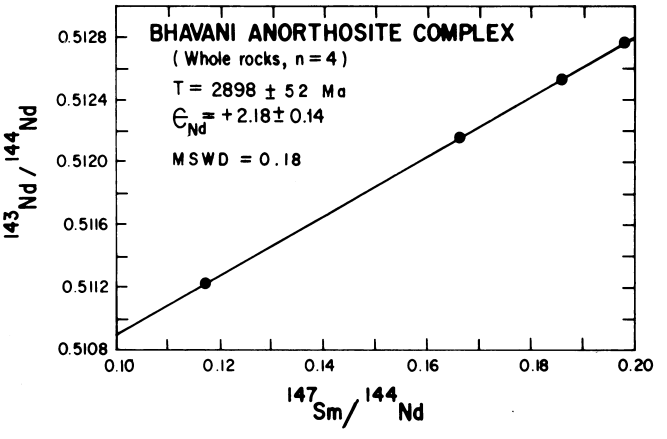

Fig. 7 Nd evolution diagram for the Bhavani whole rock samples

tions are consistent with the scheme of fractional crystallisation described for Sittampundi and Bhavani complexes (Janardhan and Leake 1975; Selvan 1981) based on data on major elements and some compatible and incompatible trace elements. Thus, it appears that in spite of significant modifications to modal layering, texture and mineralogy, the REE and many incompatible trace element compositions of the Sittampundi samples (unpublished data of the authors) reflect primary variations on the scale of sampling.

The Sittampundi anorthosites are devoid of accessory minerals like zircon, allanite etc. in contrast to some Archean anorthosites elsewhere (e.g. Fletcher et al. 1988). They show a low and restricted range of Zr (17–

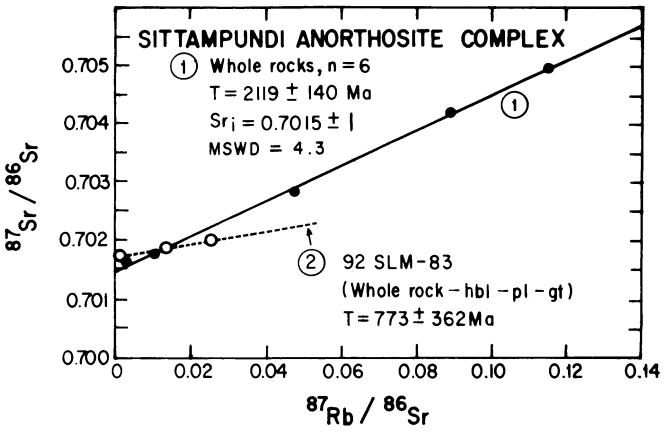

Fig. 8 Sr evolution diagram for the Sittampundi samples. Whole rocks (*1*) and whole rock - minerals (*2*)

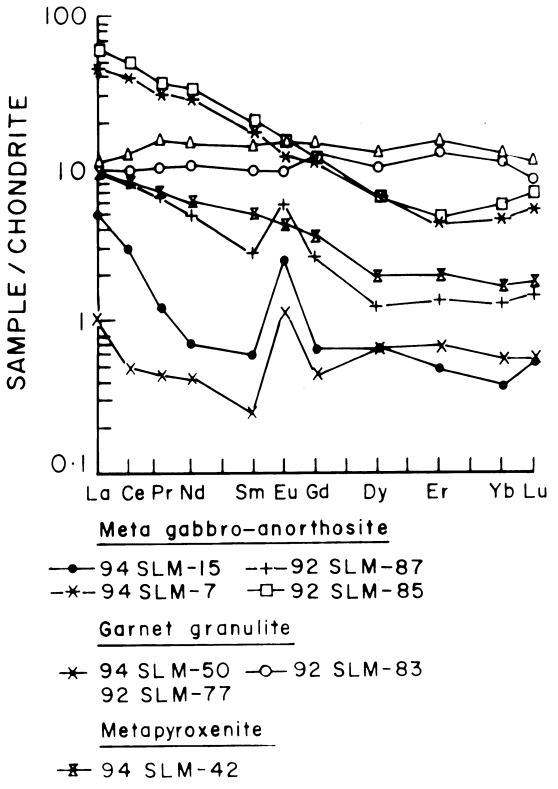

Fig. 9 Chondrite normalized rare earth element (REE) patterns for samples representing the different rock types from the Sittampundi complex

34 ppm) and lithophile elements and ratios like Rb and Rb/Sr (Table 4) that are sensitive monitors of contamination processes. We find no statistically significant correlations between Nd isotope compositions and major-trace elements such as SiO_2, MgO, Al_2O_3, Zr, Y, Nb, Ba and REE (Janardhan and Leake 1975; and unpublished data of present authors). Together with the extremely low Sr_i (0.7015 even at c. 2.0 Ga) and the positive εNd (+1.85), these geochemical features argue that the linear correlations are indeed isochrons.

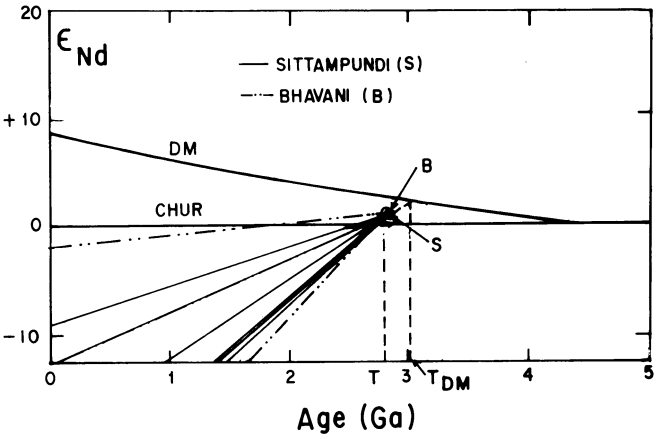

Fig. 10 Plot showing the evolution of ε_{Nd} for the Sittampundi and Bhavani samples with $^{147}Sm/^{144}Nd < 0.18$. ε_{Nd} evoluation for CHUR and DM (DePaolo 1981) are shown for comparision. The intersections for the Sittampundi samples (*S*) and Bhavani samples (*B*) indicate $\varepsilon_{Nd} > 0$ at 2.9 to 3.0 Ga (*T*) while extrapolations of S and B on to the DM evolution curve indicate older ages (T_{DM}) of ~3.1 Ga for protoliths

Apart from the agreement in their Sm-Nd isochron ages, the Sittampundi and Bhavani suites also show very similar ε_{Nd}s (+1.85 and +2.18) indicating derivation of their parental magmas from similar LREE depleted mantle sources (DM) relative to CHUR. These relationships are illustrated in Fig. 10, which shows the Nd isotopic evolution of several low $^{147}Sm/^{144}Nd$ samples (< 0.18) relative to both DM and CHUR.

Based on the foregoing discussion, we interpret the c. 2.9 Ga isochron age as representing a minimum age for the Sittampundi and Bhavani complexes. From an analogy with the Archean supracrustal rocks in the WDC, we suggest the c. 2.9 Ga ages could represent the time of M_i metamorphism of the suites. The positive ε_{Nd} values imply that the time difference between emplacement of these basic igneous rocks and their granulite grade metamorphism should be short – not more than 100 Ma. The layered complexes must therefore have been emplaced close to 3.0 Ga ago. This interpretation is consistent with the structural data (Ramadurai et al. 1975) and the geological correlations of the layered complexes and host supracrustal-gneiss units (Gopalakrishnan et al. 1975, 1990) with Archean rock associations of WDC.

Time and *P-T* conditions of M_{CSZ}

The peak pressure of 11.8 kbar recorded by the garnet granulite from Sittampundi is higher by ~2 kbar than previous estimates for mafic granulites as well as a sapphirine+cordierite paragenesis in meta-anorthosite from Sittampundi (Janardhan and Leake 1975). Such high-*P* estimates are not surprising because elsewhere in the CSZ, mylonitic garnetiferous gneisses have indicated metamorphic equilibration at pressures up to 13 kbar (cf. Drury et al. 1984). In general, *P* estimates for charnock-

ites within CSZ are at least 2 kbar higher than in the NGB (data summarised by Lal 1993).

The bimodal distribution of *P* estimates cannot be ascribed merely to geographic distribution of samples. We interpret these results as reflection of mineral reactions frozen at different times during transpressional uplift related to the steep near-isothermal decompressive *P-T* trajectory. Similar interpretations have been made in tectonically comparable scenarios elsewhere, for instance, the Triangular shear zone, Limpopo belt, S. Africa (Kamber et al. 1995) and the Napier and Rayner complexes, E. Antarctica (Harley and Hensen 1990). The steep decompression (up to 4.5 kbar) inferred in this study is broadly consistent with field and thermobarometric data in granulitic blocks flanking the CSZ, for example the uplift of the Nilgiri massif across the Bhavani and Moyar boundary shears, (Srikantappa 1993) and *P-T* trajectories for SGB (e.g. Mohan and Windley 1993).

We suggest that the range of *P* between c. 11.8–7 kbar recorded by the Sittampundi garnet granulites characterizes a post-M_1 high grade metamorphic impress (M_{CSZ}) on the rocks. This is because these estimates relate to garnet formation and breakdown reactions, and there is strong textural evidence for a late garnet paragenesis from assemblages characteristic of D_1-M_1.

The whole rock Rb-Sr isochron age of the Sittampundi anorthosite at 2119 ± 198 Ma is distinctly younger than the whole rock Sm-Nd age. By itself, the significance of this younger age would be equivocal in view of the extremely small Rb/Sr ratios of the samples defining the isochron. It, however, assumes considerable significance, as it agrees quite closely with the Sm-Nd mineral (wr-Cpx-Grt) isochron age of 2013 ± 16 Ma reported for a sample of garnet granulite (exact location unknown) from the Sittampundi complex by Snow and Basu (1986). The latter age and the substantially negative (–2.5) ε_{Nd} value given by this Sm-Nd mineral isochron would imply that the Sittampundi anorthosites were subject to a second metamorphic event nearly 1000 million years after their emplacement, which equilibrated Sr isotopes on a whole rock scale but Nd isotopes only on a mineral scale.

It is intriguing that the garnet granulite sample 92SLM-83 analysed by us gives a well defined Sm-Nd mineral isochron (wr-Pl-Hbl-Grt) corresponding to an age of *not* 2000 Ma but much younger at 726 ± 9 Ma. While the Rb-Sr mineral isochron of this sample is very imprecise (773 ± 362 Ma), it is broadly consistent with the Sm-Nd age. Since the location of the garnet granulite analysed by Snow and Basu (1986) relative to that of ours is not known,it appears that some anorthosites in the complex were isotopically re-equilibrated on a mineral scale at c. 2000 Ma, whilst some others as recently as 726 Ma. The evidence for a magmatic-metamorphic event at c. 2000 Ma in the Sittampundi region is still sparse, but that for a Neoproterozoic acitivity is quite extensive. Occurrence of anorogenic carbonatite, alkali syenite, alkali ultramafic and alkalic-calc alkalic granites emplaced between 800–600 Ma has been referred to in an earlier section. Also pertinent in this context are our recent results (unpublished) for two suites of mylonitic quartzofeldspathic gneisses (Kabilamalai gneiss) within the CSZ, proximal to Sittampundi. Much like the Sittampundi suite, these also give late Archean whole rock Sm-Nd and Rb-Sr ages of 2.76 ± 0.05 Ga and 2.78 ± 0.10 Ga respectively, but Neoproterozoic Rb-Sr isochron (Bt-Kfs-wr) ages of 730 ± 36 Ma and 620 ± 32 Ma. Thus, while the possibility of c. 2000 Ma event in the CSZ cannot yet be ruled out, the existing data indiate a much stronger and distinct thermotectonic event in the CSZ (M_{CSZ}) during the Neoproterozoic.

There can be two interpretations of our Sm-Nd mineral isochron age. Following pioneering studies elsewhere on syntectonic garnets (Jagoutz 1988; Cohen et al. 1988; Vance and O'Nions 1990; Thoni and Jagoutz 1992), the 726 ± 9 Ma age for 92SLM-83 may date the prograde M_{CSZ} paragenesis. However, considering the steep decompressional *P-T* path and the uncertainties in the closure temperature (T_c) for Sm-Nd in garnets (e.g. c. 900°C, Cohen et al. 1988; 480–600°C, Mezger 1990), the 726 Ma age could relate to a stage in the retrogression implying cooling through a specific T_c. Since the garnets studied are Prp-Alm, a reasonable T_c would be c. 900–700°C (based on Cohen et al. 1988, $\sim$900°C for Prp in eclogites) and in the light of *P-T* estimates presented here, our preferred interpretation is that the 726 ± 9 Ma age relates to a near-peak stage of M_{CSZ} metamorphism.

Tectonic evolution and significance of CSZ

As the layered complexes are undoubtedly of Archean age, the CSZ cannot be a Proterozoic collapsed marginal basin as visualised by Drury et al. (1984). The results presented herein characterize the CSZ as an Archean crustal segment reworked during the Proterozoic, most intensely during the Neoproterozoic.

Interestingly, the layered complexes do not record evidence for Nd isotopic equilibration at 2.5 Ga, an event very widespread in the NGB. The preservation of older isotopic signatures (2.9 Ga) may be due to the anhydrous state of these suites at 2.5 Ga as a consequence of their early high-grade metamorphism at c. 2.9 Ga. Alternatively, we suggest that the CSZ may include allochthonous terrane(s) accreted to the Dharwar craton later than 2.5 Ga but prior to the Palaeoproterozoic (2.1–2.0 Ga) since contemporaneous thermal events are recorded throughout the NGB and adjoining WDC and EDC. More geological and geochronological data will be required to assess this possibility.

The 2.9 Ga age of the Sittampundi-Bhavani complexes is comparable to that of the Messina complex, Limpopo Mobile Belt, S. Africa (Barton et al. 1979), which is significant in the light of the similarity in their tectonic environments (Ashwal 1993). However, unlike Limpopo, the evidence for a c. 2.0 Ga tectonometamorphic event in the CSZ, is yet only marginal.

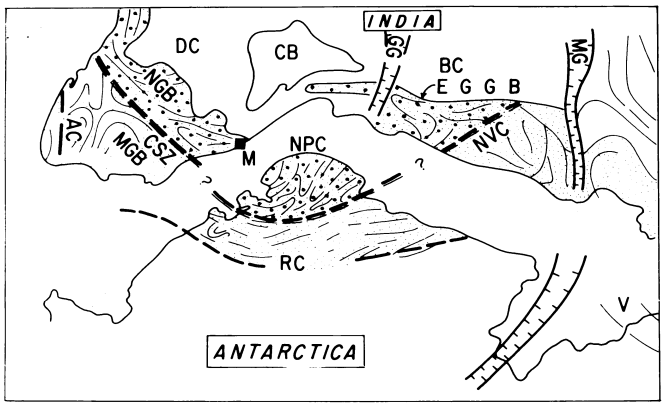

Fig. 11 A Proterozoic reconstruction of India and east Antarctica (Chetty 1995) showing the correlation of the CSZ and the boundary between the Napier (*NPC*) and Rayner (*RC*) complexes

Our data support the recent interpretations of age data on the south Indian granulite terrain, which suggest that the CSZ could be a prominent Archean-Proterozoic terrane boundary (e.g. Harris et al. 1994; Jayananda et al. 1995). The strong decompressive *P-T* history of up to 4.5 kbar for the CSZ during the Neoproterozoic M_{CSZ} described herein is quite relevant to correlations within the eastern Gondwana Supercontinent. In general, many Proterozoic granulite terrains both from southern India and its immediate neighbours in Gondwanian reconstructions (such as Sri Lanka, Madagascar and E. Antarctica) show similar decompression histories ascribed to their rapid exhumation following Neoproterozoic collisions around 1000 Ma and 550 Ma (e.g. Nicollet 1988; Schumacher et al. 1990; Harley and Hensen 1990; Srikantappa 1993; Mohan and Windley 1993). Apart from the *P-T* history of granulites, the CSZ is also comparable to these terrains in terms of its transpressional tectonic regime (e.g. Drury et al. 1984; Chetty and Bhaskar Rao 1996).

Of particular interest is the link between the CSZ and the boundary between the Archean Napier and the Proterozoic Rayner complexes of E. Antarctica proposed recently by Harris et al. (1994) and Chetty (1995), Fig. 11. As summarised by Harley and Hensen (1990) and S.L. Harley (1996, personal communication), granulites at several places along the Napier-Rayner boundary show textures indicating significant isothermal decompression, but unlike the rocks of the CSZ, deformation and granulite matamorphism there are dated at 1100 Ma and 550 Ma and granite emplacement at c. 770 Ma. Since these ages do not tally with those available for the CSZ, the proposed link between these Archean-Proterozoic boundaries is not obvious. Nevertheless, the suggestion remains an interesting possibility. More detailed geochronological studies on the CSZ and a critical assessment of the proposed extension of CSZ into the Eastern Ghats belt (Drury and Holt 1980) will be significant because both 1100 Ma and 550 Ma metamorphisms have been documented in the Eastern Ghats belt.

Concluding statements

1. The Sittampundi and Bhavani complexes give concordant Sm-Nd whole rock isochron ages and ε_{Nd} of c. 2.9 Ga and +2.0, respectively.

2. The suites suffered at least two episodes of high grade metamorphism around 2.9 Ga and 0.73 Ga, the latter relating to the transpressional tectonic events culminating in shearing along the Cauvery shear zone. The possibility of a metamorphic impress at c. 2.0 Ga can not yet be ruled out.

3. The Cauvery shear zone represents a prominent Archean-Proterozoic boundary in the southern granulite terrain of south India.

Acknowledgements We appreciate valuable help from Dr. Anil Kumar during isotopic analyses, Drs. R. Natarajan and S. Moeen in microprobe analyses, Dr.V. Balaram in REE analyses and Dr. T.V. Sivaraman in computations with *P-T* CALC (Computer Program coded by T.V.Sivaraman based on Lal, 1993) and TWEEQU. The critical reviews and comments of referees, Prof. L.D. Ashwal (S. Africa) and Prof. S.L. Harley (Scotland) were very useful in improving the original manuscript. We thank the Director, NGRI for support and permission to publish this work. Mr. P.V. Swamy and Ms. Nancy Rajan prepared the manuscript.

References

Anil Kumar, Gopalan K (1992) Precise Rb-Sr age and enriched mantle source of the Sevathur carbonatites, Tamil Nadu. Curr Sci 60: 653–655

Anil Kumar, Bhaskar Rao YJ, Sivaraman TV, Gopalan K (1996) Sm-Nd ages of Archaean metavolcanics of the Dharwar craton, South India. Precambrian Res (in press)

Ashwal LD (1993) Anorthosites, Springer-Verlag, Berlin Heidelberg New York

Ashwal LD, Myers JS (1994) Archaean anorthosites. In: Condie KC (ed) Archaean crustal evolution. (Developments in Precambrian geology, vol 11) Elsevier, Amsterdam, pp 315–356

Barton JM Jr, Fripp REP, Harrocks PC, McLean N (1979) The geology, age, and tectonic setting of the Messina Layered Intrusion, Limpopo Mobile Belt, southern Africa. Am J Sci 279: 1108–1134

Berman RG (1990) Mixing properties of Ca-Mg-Fe-Mn garnets. Am Mineral 75: 328–344

Berman RG (1991) Thermobarometry using multiequilibrium calculations: a new technique with petrologic applications. Can Mineral 29: 833–855

Berman RG, Arnovich LY (1993) Optimised standard state and solution properties of olivine, orthopyroxene, garnet, cordierite, and biotite (abstract). Geol Soc Am Abstr Program 25:A100

Berman RG, Koziol AM (1991) Ternary excess properties of grossular-pyrope-almandine garnets and their influence in geothermobarometry. Am Mineral 76: 1223–1231

Bhaskar Rao YJ, Sivaraman TV, Pantulu GVC, Gopalan K, Naqvi SM (1992) Rb-Sr ages of late Archean metavolcanics and granites, Dharwar craton, South India and evidence for Early Proterozoic thermotectonic event(s). Precambrian Res 59: 145–170

Bohlen SR, Wall VJ, Boetcher AC (1983) Experimental investigation and application of garnet granulite equilibria. Contrib Mineral Petrol 83: 52–61

Chetty TRK (1995) A correlation of Proterozoic shear zones between Eastern Ghats, India, and Enderby land, East Antarctica. In: Yoshida S, Santosh M (eds) India and Antarctica during the Precambrian. Mem Geol Soc India 34: 205–220

Chetty TRK, Bhaskar Rao YJ (1996) The Cauvery shear zone in the southern granulite terrain, south India: evidence for Neoproterozoic westward thrusting. J Geol Soc London (submitted)

Choudhury AK, Harris NBW, Van Carlsteren P, Hawksworth CJ (1992) Pan African charnockite formation in Kerala, South India. Geol Mag 129: 257–267

Christensen JN, Selverstone J, Rosenfeld JI, DePaolo DJ (1994) Correlation by Rb-Sr geochronology of garnet growth histories from different structural levels within the Tauern Window, Eastern Alps. Contrib Mineral Petrol 118: 1–12

Cohen AS, O'Nions RK, Siegnenthaler R, Griffin WJ (1988) Chronology of the pressure-temperature history recorded by a granulite terrain. Contrib Mineral Petrol 98: 303–311

Dahl PS (1980) The thermal compositional dependence of Fe^{+2}-Mg distributions between co-existing garnet and pyroxene; applications to geothermometry. Am Mineral 65: 852–866

DePaolo DJ (1981) Neodymium isotopes in the Colorado Front Range and crust-mantle evolution in the Proterozoic. Nature 291: 193–196

DePaolo DJ (1988) Neodymium isotope geochemistry: an introduction. Springer-Verlag, Berlin Heidelberg New York

Drury SA, Holt RW (1980) The tectonic framework of the south Indian craton: a reconnaissance involving LANDSAT imagery. Tectonophysics 65:T1–T15

Drury SA, Harris NBW, Holt RW, Reeves-Smith GJ, Wightman RT (1984) Precambrian tectonics and crustal evolution in south India. J Geol 92: 3–20

Eckert JO Jr, Newton RC, Kleppa OJ (1991) $\triangle$H of reaction and recalibration of garnet-pyroxene-quartz geothermometers in CMAS system by solution calorimetry of stoichiometric mineral mixes. Am Mineral 76: 148–160

Ellis DJ, Green DH (1979) An experimental study of the effect of Ca upon garnet-clinopyroxene exchange equilibria. Contrib Mineral Petrol 71: 13–22

Fitzsimons ICW, Harley SL (1994) The influence of retrograde cation exchange on granulite *P-T* estimates and a convergence technique for the recovery of peak metamorphic conditions. J Petrol 35: 543–576

Fletcher IR, Rosman KJR (1982) Precise determination of initial Nd from Sm-Nd isochron data. Geochim Cosmochim Acta 46: 1983–1987

Fletcher IR, Rosman KJR, Libby WG (1988) Sm-Nd, Pb-Pb and Rb-Sr geochronology of the Manfred complex, Mount Narryer, Western Australia. Precambrian Res 38: 343–354

Fuhrman ML, Lindsley DH (1988) Ternary-feldspar modeling and thermometry. Am Mineral 73: 201–215

Ganguly JB, Saxena SK (1989) Mixing properties of aluminum silicate garnets: constraints from natural and experimental data and application to geothermobarometry. Am Mineral 69: 88–97

Gopalakrishnan K, Suguvanam EB, Venkata Rao V (1975) Are there rocks older than Dharwars? A reference to rocks in Tamil Nadu. Indian Mineral 16: 26–34

Gopalakrishnan M, Venkata Rao V, Viswanathan TV (1990) Role of palaeosutures in the evolution of southern Indian granulite terrain. In: Group discussion on suture zones; young and old (abstract). Wadia Inst Himalayan Geol, Dehra Dun, India, pp 55–60

Harley SL (1984a) Experimental study of the partitioning of Fe and Mg between garnet and orthopyroxene. Contrib Mineral Petrol 86: 359–373

Harley SL (1984b) The solubility of alumina in orthopyroxene coexisting with garnet in FeO-MgO-Al_2O_3-SiO_2 and CaO-FeO- MgO-Al_2O_3-SiO_2. J Petrol 25: 665–696

Harley SL (1988) Proterozoic granulites from the Raucs Group, East Antarctica. I. Decompressional pressure-temperature paths deduced from mafic and felsic gneisses. J Petrol 29: 1059–1095

Harley SL, Hensen BJ (1990) Archaean and Proterozoic high grade terrains of East Antarctica (40–80°E): a case study of diversity in granulite facies metamorphism. In: Ashworth JR, Brown M (eds) High temperature metamorphism and crustal anatexis. Unwin Hyman, pp 320–364

Harris NBW, Santosh M, Taylor PN (1994) Crustal evaluation in south India: constraints from Nd isotopes. J Geol 102: 139–150

Hatton CJ, Von Gruenewaldt (1990) Early Precambrian layered intrusions. In: Hall RP, Hughes DJ (eds) Early Precambrian basic magmatism. Blackie, London, pp 56–81

Henderson P, Fishlock SJ, Laul JC, Cooper TD, Conard RL, Boynton WV, Schmitt RA (1976) Rare earth element abundances in rocks and minerals from the Fiskenaesset complex, West Greenland. Earth Planet Sci Lett 30: 37–49

Hensen BJ, Zhou B (1995) A Pan-African granulite facies metamorphic episode in Prydz Bay, Antarctica: evidence from Sm-Nd garnet dating. Aust J Earth Sci 42: 249–258

Holland TJB, Powell R (1990) An enlarged and updated internally consistent thermodynamic data set with uncertainties and correlations: the system K_2O-Na_2O-CaO-MgO-MnO-FeO-Fe_2O_3-Al_2O_3-TiO_2-SiO_2-C-H_2-O_2. J Metamorphic Geol 8: 89–124

Jagoutz E (1988) Nd and Sr systematics in an eclogite xenolith from Tanzania: evidence for frozen mineral equilibria in continental lithosphere. Geochim Cosmochim Acta 31: 1285–1292

Janardhan AS, Leake BE (1975) The origin of the meta-anorthositic gabbros and garnetiferous granulites of the Sittampundi complex, Madras, India. J Geol Soc India 6: 391–408

Janardhan AS, Jayananda M, Shankara MA (1994) Formation and tectonic evolution of granulites from the Biligiri Rangan and Nilgiri Hills, S. India: geochemical and isotopic constraints. J Geol Soc India 44: 27–40

Jayananda M, Janardhan AS, Sivasubramanian P, Peucat JJ (1995) Geochronologic and isotopic constraints on granulite formation in the Kodaikanal area, southern India. In: Yoshida M, Santosh M (eds) India and Antarctica during the Precambrian. Mem Geol Soc India 34, pp 373–390

Kamber BS, Kramers JD, Napier R, Cliff RA, Rollinson HR (1995) The Triangle shear zone, Zimbabwe, revisited: new data document an important event at 2.0 Ga in the Limpopo Belt. Precambrian Res 70: 191–213

Korsch MJ, Gulson BL (1986) Nd and Pb isotopic studies of an Archaean layered mafic-ultramafic complex, Western Australia, and implications for mantle heterogeneity. Geochim Cosmochim Acta 50: 1–10

Kretz R (1983) Symbols for rock-forming minerals. Am Mineral 68: 277–279

Krogh EJ (1988) The garnet-clinopyroxene Fe-Mg geothermometer reinterpretation of existing experimental data. Contrib Mineral Petrol 99: 44–48

Lal RK (1993) Internally consistent recalibrations of mineral equilibria for geothermobarometry involving garnet-orthopyroxene-plagioclase-quartz assemblages and their application to the south Indian granulites. J Metamorphic Geol 11: 855–866

Lee HY, Ganguly JB (1988) Equilibrium compositions of co-existing garnet and orthopyroxene: experimental determinations in the system FeO-MgO-Al_2O_3-SiO_2 and applications. J Petrol 29(1):93–113

Mahabaleswar B, Jayananda M, Peucat JJ, Sadakshara Swamy N (1995) Archean high grade gneiss complex for Satnur-Holegur Sivasamudram areas, Karnataka, southern India: petrogenesis and crustal evolution. J Geol Soc India 45: 33–50

Mezger K (1990) Geochronology in granulites. In: Vielzeuf D, Vidal P (eds) Granulites and crustal evolution. Kluwer Academic, Netherlands, pp 431–470

Moecher BP, Essene EJ, Anovitz LM (1988) Calculation and application of clinopyroxene-garnet-plagioclase-quartz geobarometers. Contrib Mineral Petrol 100: 92–106

Mohan A, Windley BF (1993) Crustal trajectory of sapphirine bearing granulites from Ganguvarpatti,South India–evidence for isothermal decompression path. J Metamorphic Geol 11: 867–878

Newton RC (1983) Geobarometry of high-grade metamorphic rocks. Am J Sci 293A:1–28

Newton RC, Perkins D (1982) Thermodynamic calibration of geobarometers based on the assemblages garnet-plagioclase- orthopyroxene-clinopyroxene-quartz. Am Mineral 67: 203–222

Nicollet (1990) Crustal evolution of granulites of Madagascar. In: Vielzeuf D, Vidal Ph (eds) Granulites and crustal evolution (NATO ASI Series-C, 311) Kluwer Academic, Netherlands, pp 291–311

Perkins D, Chipera SL (1985) Garnet-clinopyroxene-plagioclase-quartz-barometry: refinement and application to the English River subprovince and the Minnesota River Valley. Contrib Mineral Petrol 84: 69–80

Peucat JJ, Vidal P, Bernard-Griffiths J, Condie KC (1989) Sr, Nd, and Pb isotopic systematics in the Archean low- to high-grade transition zone of southern India: syn-accretion versus post-accretion granulites. J Geol 97: 537–550

Peucat JJ, Mahabaleshwar R, Jayananda M (1993) Age of younger tonalitic magmatism and granulite metamorphism in the south Indian transition zone, Krishnagiri area, comparison with older Peninsular gneiss from the Gorur-Hassan area. J Metamorphic Geol 11: 879–888

Phinney WC, Morrison DA, Maczuga DE (1988) Anorthosites and related megacrystic units in the evolution of Archean crust. J Petrol 29: 1283–1323

Powell R (1978) The thermodynamics of pyroxene geotherms. Phil Trans Roy Soc Lond, 288A:457–469

Provost A (1990) An improved diagram for isotope data. Chem Geol Isot Geosci 80: 85–89

Raith M, Raase P, Ackermand D, Lal RK (1983) Regional geothermobarometry in the granulite facies terrain of south India. Trans R Soc Edinburgh Earth Sci 73: 221–244

Ramadurai S, Sankaran M, Selvan TA, Windley BF (1975) The stratigraphy and structure of the Sittampundi complex, Tamil Nadu, India. J Geol Soc India 16: 409–414

Ramakrishnan M (1993) Tectonic evolution of the granulite terrains of southern India. Mem Geol Soc India 25: 35–44

Reddy BM, Janardhan AS, Peucat JJ (1995) Geochemistry, age and origin of alkaline and ultramafic rocks of Salem, Tamil Nadu, South India. J Geol Soc India 45: 251–262

Sandiford M, Powell R, Martin SF, Perera LRK (1988) Thermal and baric evolution of garnet granulites from Sri Lanka. J Metamorphic Geol 6: 273–304

Schumacker R, Schenk V, Raise P, Vitinage PW (1990) Granulite facies metamorphism of metabasic and metapelitic rocks in the Highland series of Sri Lanka. In: Ashworth JR, Brown M (eds) High temperature metamorphism and crustal anatexis. Unwin Hyman, pp 235–271

Selvan TA (1981) Anorthosite-gabbro-ultramafic complex around Gobihchettypalayam, Tamil Nadu and their possible relation to Sittampundi type anorthosite complex (unpublished). PhD thesis, Univ Mysore, Mysore, India

Snow J, Basu AR (1986) The Sittampundi complex, S. India – Nd isotopic chronology of lower crustal granulites (abstract). EOS Trans Am Geophys Union 67: 400

Srikantappa C (1993) High pressure charnockites of the Nilgiri Hills, southern India. In: Radhakrishna BP (ed) Continental crust of south India. Mem Geol Soc India 25: 95–111

Subba Rao TV, Narayana BL, Gopalan K (1994) Rb-Sr age of the Sivamalai alkaline complex, India. Proc Indian Acad Sci Earth Planet Sci 103: 428–437

Subramanian AP (1956) Mineralogy and petrology of the Sittampundi complex, Salem district, Madras State, India. Bull Geol Soc Am 67: 317–390

Thoni M, Jagoutz E (1992) Some new aspects of dating eclogites in orogenic belts: Sm-Nd, Rb-Sr and Pb-Pb isotopic results from the Austro-Alpine Saoalpe and Koralpe. Geochim Cosmochim Acta 56: 347–368

Thost DE, Hensen BJ, Motoyoshi Y (1991) Two-stage decompression in garnet-bearing mafic granulites from Sostrene Island, Prydz Bay, East Antarctica. J Metamorphic Geol 9: 245–256

Vance D, O'Nions RK (1990) Isotopic chronometry of zoned garnets: growth kinetics and metamorphic histories. Earth Planet Sci Lett 97: 227–240

Wells PRA (1977) Pyroxene thermometry in simple and complex systems. Contrib Mineral Petrol 62: 129–139

Wells PRA (1979) Chemical and thermal evolution of Archaean sialic crust, southern West Greenland. J Petrol 20: 187–226

Willamson JH (1968) Least-squares fitting of a straight line. Can J Phys 46: 1845–1849

Windley BF, Herd RK, Bowden AA (1973) The Fiskenaesset complex, West Greenland. I. A preliminary study of the stratigraphy, petrology and whole rock chemistry from Qeqertarssuatsiaq. Bull Gronl Geol Unders: 106: pp 80